



# A dual-tracer approach to estimate upwelling velocity in coastal Southern California



William Z. Haskell II\*, Douglas E. Hammond, Maria G. Prokopenko

Earth Sciences Dept., University of Southern California, Los Angeles, CA 90089, USA

## ARTICLE INFO

### Article history:

Received 19 December 2014  
 Received in revised form 18 March 2015  
 Accepted 9 April 2015  
 Available online 28 April 2015  
 Editor: J. Lynch-Stieglitz

### Keywords:

upwelling  
 particle export  
 radioactive tracers

## ABSTRACT

The distribution of the cosmogenic radionuclide  $^7\text{Be}$  ( $t_{1/2} = 53\text{d}$ ) in the surface ocean has previously been used to estimate upwelling velocity in the open ocean. However, the loss of  $^7\text{Be}$  to particle export has limited this approach in high particle density environments like the continental margins. In this study, we combine a mass balance of  $^7\text{Be}$  with a  $^{234}\text{Th}$  budget in the surface ocean to constrain the loss of  $^7\text{Be}$  to particle sinking at the San Pedro Ocean Time-series (SPOT) in the inner Southern California Bight during spring 2013. Upwelling velocities (all in  $\text{m d}^{-1}$ ) determined from the  $^7\text{Be}$  mass balance were observed to increase from  $0.5 \pm 0.6$  in January to  $2.5 \pm 1.3$  in May, then decrease to  $1.2 \pm 0.5$  in June. These results agree within uncertainty with upwelling velocities derived from the monthly Bakun Upwelling Index, which ranged from 0.1 to  $2.8 \text{ m d}^{-1}$ , supporting the pressure-field-based approach. Evidence from a heat budget and the nutrient distribution over the course of the study supports that the upwelling signal at SPOT (20 km offshore) is not transported from coastal upwelling near shore, but instead is dominantly a local signal, likely driven by wind-stress curl.

© 2015 Elsevier B.V. All rights reserved.

## 1. Introduction

The inventory and distribution of the cosmogenic radionuclide,  $^7\text{Be}$  ( $t_{1/2} = 53\text{d}$ ), in the surface ocean has been used as a tracer of circulation, including upwelling velocity into the upper thermocline (Kadko and Johns, 2011; Haskell II et al., 2015). Because of its typically small magnitude, upwelling velocity has been notoriously difficult to measure and most chemical tracers (i.e.  $^{14}\text{C}$ ,  $\delta^{13}\text{C}$ , Apparent Oxygen Utilization (AOU),  $\delta^3\text{He}$ , and  $\text{pCO}_2$ ) previously used to estimate its magnitude have long lifetimes in the water column (Broecker and Peng, 1982; Broecker et al., 1978; Quay et al., 1983; Wanninkhof et al., 1995; Klein and Rhein, 2004). The mean lifetime of  $^7\text{Be}$  in the water column is on the order of weeks to months, thus it is able to capture the dynamic range of upwelling over the timescale of biological production. Previous applications of this approach have been limited to open ocean regimes because the loss of  $^7\text{Be}$  adsorbed onto particles must be better constrained in higher particle flux environments (Haskell II et al., 2015).

Coastal upwelling zones are some of the most productive regions in the world's oceans, accounting for 30–50% of global marine primary productivity (Jahnke, 1996). Future climate forcing may affect upwelling patterns and water column stratification

(Levitus et al., 2001; Barnett et al., 2001). In order to better understand the control that upwelling of deep-water nutrients has on marine productivity over the continental margins and how these ecosystems may respond to future climate change, constraints on upwelling velocities on the timescale of bloom evolution are needed in these highly productive surface ocean regimes.

The Southern California Bight (SCB) is located between Point Conception to the North and the US/Mexico border to the South (Fig. 1). From winter to summer, the surface currents increase in magnitude from the northwest as a portion of the California Current (CC) splits off into the inner SCB. The combined effect of the Coriolis acceleration and wind stress drive net offshore transport of surface water, causing both near-shore coastal upwelling and wind stress curl-driven upwelling (as defined by Rykaczewski and Checkley, 2008; Jacox and Edwards, 2011). This effect is strongest during spring and early summer. During the late summer and early fall, prevailing wind directions shift, and the Southern California Countercurrent (SCC) begins to flow from the Southeast against the CC. During fall and early winter months, the SCC dominates the surface current flow, upwelling velocity is minimal and the surface ocean returns to a more eddy diffusion-dominated transport system. This seasonal upwelling pattern is reflected in the Bakun Upwelling Index, an estimate of offshore Ekman transport driven by geostrophic wind stress, based on measurements of atmospheric pressure fields (Bakun, 1973; Schwing et al., 1996). However, the Bakun Upwelling Index may reflect large-scale off-shore

\* Corresponding author. Tel.: +1 240 687 0772; fax: +1 213 740 8801.

E-mail address: whaskell@usc.edu (W.Z. Haskell).

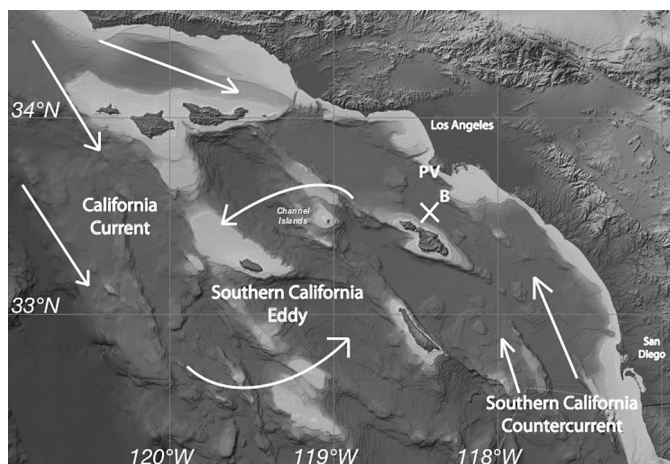


**Fig. 1.** Map of the study area including major surface currents in the region. The location of this study (San Pedro Ocean Time-series (SPOT)) is marked by the white 'X'. The Palos Verdes station is marked with the letters, 'PV.' NOAA buoy 46222 is marked with a 'B' (NGDC, 2011).

mass transport, rather than local upwelling dynamics, since it is derived from pressure gradients over large distances ( $\sim 300$  km).

In this study, we use a dual-tracer approach to estimate upwelling velocity in the upper thermocline in San Pedro Basin from January to June of 2013. Measurements of  $^7\text{Be}$  inventory, primarily sensitive to loss by upwelling, are combined with those of  $^{234}\text{Th}$ , primarily sensitive to particle export, to apply these tracers in a high particle flux environment. These measurements are part of a larger effort to characterize the biological response to upwelling, the Upwelling Regime In-Situ Ecosystem Efficiency (Up.R.I.S.E.E.) study, located at the San Pedro Ocean Time-series (SPOT) station ( $33^\circ 33' \text{N}$ ,  $118^\circ 24' \text{W}$ ).

## 2. Material and methods

### 2.1. Beryllium-7

Two depths were sampled for  $^7\text{Be}$  at the SPOT hydrostation (Fig. 1), approximately every two weeks from January to June 2013. Samples from the mixed layer (40 L) and 10 m below the mixed layer (80 L), as determined from temperature profiles during CTD descent, were taken with a CTD equipped with twelve, 12 L Niskin bottles. In this study, we define the base of the mixed layer as the depth where the temperature differs from the surface value by  $0.5^\circ\text{C}$ . Water from each depth was transferred into 10 L cubitainers and taken back to the lab. Each cubitainer was spiked with a known amount of  $^9\text{Be}$  used as a yield tracer and equilibrated for  $\sim 24$  h, then acidified with 12.5 mL of 10 N HCl to pH of  $< 2$  and bubbled with  $\text{N}_2$  for at least one hour to drive off all inorganic carbon.  $\text{FeCl}_2$  (50 mg) was added to each cubitainer and allowed to mix thoroughly for one hour before 12.5 mL of  $\text{NH}_4\text{OH}$  was added to raise the pH and co-precipitate  $^7\text{Be}$  and  $\text{Fe}(\text{OH})_3$ . Each cubitainer was allowed to settle for 2 days,  $\sim 8$  L of solution was decanted off the top, and then the remaining solution containing the precipitate from all cubitainers for a single depth was combined into a single centrifuge tube and centrifuged down to fit into a counting tube.

Each sample was counted on an Ortec low-background intrinsic Germanium (Ge) gamma detector (well-type, 100cc active volume).  $^7\text{Be}$  has a readily identifiable gamma peak at 478 keV. Detection efficiency was determined by measuring gammas emitted by standards of known activity. The effect for sample geometry was found by counting a solution of known gamma activity in sample tubes filled to different heights. The uncertainty of extraction efficiency and the detector efficiency was in all cases smaller than the

statistical counting error and the uncertainty in the blank. Recovery yield of  $^9\text{Be}$  was measured following gamma counting by first re-dissolving the  $\text{Fe}(\text{OH})_3$  precipitate in a 10% nitric acid matrix, equilibrating with BIO-RAD AG 50W-X12 cation-exchange resin to remove Fe (von Blanckenburg et al., 1996), and then analyzing the Be eluate on a Microwave Plasma Optical Emission Spectrometer (MP-OES) to measure recovered  $^9\text{Be}$ . This recovery yield was used in all  $^7\text{Be}$  calculations to correct for methodological efficiency (Mean: 0.88; Standard Deviation: 0.13). All water column  $^7\text{Be}$  activities are reported in Table 1.

The activity of  $^7\text{Be}$  in rain ( $A_{\text{Be}}$ ) was measured on rain collected by bucket on the rooftop of one of the tallest buildings ( $\sim 6$  stories tall; separated from other tall buildings) on the USC campus intermittently throughout the study period. The same  $\text{Fe}(\text{OH})_3$  co-precipitation and isotopic dilution procedures used to process seawater samples were performed on the rainwater, and they were counted on the same gamma detectors (average activity =  $201 \text{ dpm L}^{-1}$ ; Table S1).

### 2.2. Thorium-234

Vertical profiles from the surface to 200 m were collected for thorium via Niskin/CTD on every cruise. Ten liters were sampled at eight to ten depths, chosen based on fluorescence measured during the CTD's descent. The analysis of each sample follows the method published in Haskell II et al. (2013). An isotope dilution method using a  $^{229}\text{Th}$  spike of known activity and co-precipitation with  $\text{MnO}_2$  was used to measure  $^{234}\text{Th}$  (Rutgers van der Loeff and Moore, 1999; Mean Yield: 0.83, Standard Deviation: 0.15). The  $^{234}\text{Th}$  deficit relative to its parent isotope,  $^{238}\text{U}$ , was calculated by trapezoidal integration of the profile.  $^{238}\text{U}$  activity was calculated as a function of salinity ( $^{238}\text{U}$  activity ( $\text{dpm L}^{-1}$ ) =  $0.07097 * \text{Salinity}$ ; Chen et al., 1986).

### 2.3. Sediment traps

During 4 cruises, one surface-tethered drifting sediment trap of the Particle-Interceptor-Traps (PITs) design was deployed at 100 m with a total surface area of  $0.0851 \text{ m}^2$  (Knauer et al., 1979). The trap had 12 collection tubes with an aspect ratio of 6.4 and  $1 \text{ cm} \times 1 \text{ cm}$  baffles fitted into the opening of the tubes. Funnel with centrifuge tubes were attached into the base of each trap tube. The centrifuge tube contained a brine solution of NaCl (in excess of sea water by 5 ppt) that was poisoned with 3% formaldehyde and buffered with disodium tetraborate. Deployments lasted  $\sim 24$  h. After recovery, each of the twelve centrifuge tubes were put through a series of centrifuging/decanting/diluting cycles to remove all salts, then combined onto Whatman Nuclepore polycarbonate membrane ( $0.4 \mu\text{m}$ ) filters and dried at room temperature. All material from each trap was folded and put in a single counting tube and counted on the same counters as the other  $^7\text{Be}$  and  $^{234}\text{Th}$  samples.

### 2.4. Nutrients

Dissolved nutrient samples were collected via Niskin bottles at 12 depths from the surface to 400 m and filtered through  $0.8/0.2 \mu\text{m}$  syringe filters into two Nalgene bottles for each depth. One was used for silica and phosphate analyses done colorimetrically at USC with a Hitachi UV/vis-spectrophotometer (Parsons et al., 1984). Nitrate samples were collected in acid-washed bottles and frozen at  $-20^\circ\text{C}$ , until analysis. Nitrate concentrations were determined by converting nitrate to  $\text{N}_2\text{O}$  (Sigman et al., 2001) and quantifying the amount of  $\text{N}_2\text{O}$  as integrated sample areas on an Isotope Ratio Mass Spectrometer (IRMS) in the D. Sigman lab at Princeton University. Prior to analyses, nitrite was chemically removed from samples (Granger and Sigman, 2009).

Download English Version:

<https://daneshyari.com/en/article/6428339>

Download Persian Version:

<https://daneshyari.com/article/6428339>

[Daneshyari.com](https://daneshyari.com)